# Target site selection for an RNA-cleaving catalytic DNA

**Murray J. Cairns, Toni M. Hopkins, Craig Witherington, Li Wang, and Lun-Quan Sun***

*Johnson and Johnson Research Laboratories, GPO Box 3331, Sydney 2001, Australia. *Corresponding author (e-mail: sun@angis.su.oz.au).*

Received 24 August 1998; accepted 18 March 1999

**A small catalytic DNA, known as the 10–23 DNA enzyme or deoxyribozyme, has been shown to efficiently hydrolyze RNA at purine-pyrimidine (R-Y) junctions in vitro. Although these potentially cleavable junctions are ubiquitous, they are often protected from deoxyribozyme activity by RNA secondary structure. We have developed a multiplex cleavage assay for screening the entire length of a target RNA molecule for deoxyribozyme cleavage sites that are efficient, both in terms of kinetics and accessibility. This strategy allowed us to simultaneously compare the RNA cleaving activity of 80 deoxyribozymes for a model target gene (*HPV16 E6*), and an additional 60 deoxyribozymes against the rat c-*myc* target. The human papilloma virus (HPV) target was used primarily to characterize the multiplex system and determine its validity. The c-*myc* target, coupled with a smooth muscle cell proliferation assay, allowed us to assess the relationship between in vitro cleavage efficiency and c-*myc* gene suppression in cell culture. The multiplex reaction approach streamlines the process of revealing effective deoxyribozymes in a functional assay and provides accessibility data that may also be applicable to site selection for other hybridization-based agents.**

Keywords: deoxyribozyme, oligonucleotide, DNAzyme, secondary structure, RNA accessibility



The 10–23 general purpose RNA-cleaving DNA enzyme, or deoxyribozyme, was derived by in vitro selection from a combinatorial library of DNA sequences able to cleave a short HIV target RNA[1], and has the potential to bind and cleave any target RNA that contains a purine-pyrimidine junction. The Watson-Crick base pairing that confers substrate recognition and binding of the deoxyribozyme also allows specificity to be modified for any target. In addition to its broad specificity, this DNA enzyme has been shown to catalyze the cleavage of RNA with high efficiency under simulated physiologic conditions[1]. These features are attractive for application in gene inactivation strategies.

Given the wide range of potential cleavage sites for this molecule, finding the optimal deoxyribozyme for therapeutic use is not trivial. For simple oligonucleotides, the reaction kinetics are relatively sequence dependent, but for longer substrates, the secondary structure of the target RNA profoundly influences cleavage efficiencies. For some RNA molecules, this may be further complicated by tertiary structure and protein binding in vivo.

Previous attempts to screen RNA targets for accessible sites have used a variety of strategies. In the case of conventional antisense oligodeoxynucleotides (ODNs), large oligonucleotide arrays have been used to map sites of target RNA hybridization[2]. An alternative approach used RNase H activity as an assay for mapping target sites accessible to hybridization with random and semirandom ODNs[3–6]. A nonrandom variation of this strategy uses DNaseI digestion of double-stranded template DNA to generate target-specific oligonucleotides[7]. Assuming an RNase H–dependent mechanism in vivo, these functional assays may be better for selecting molecules for cellular applications because they indicate both hybridization strength and enzyme activation. Target-site selection for catalytic RNA has also been accomplished. In the case of the hammerhead ribozymes, target-site selection can be accomplished using pools of molecules with randomized hybridizing arms[8]. Similarly, randomization of the internal guide sequence of the group I intron can select, from a long substrate, sites that are accessible for *trans* cleavage by this ribozyme[9].

We describe here a multiplex cleavage assay for screening the entire length of a target RNA molecule for deoxyribozyme cleavage sites that are efficient, both in terms of kinetics and accessibility.

## Results

Deoxyribozyme design. All deoxyribozyme oligonucleotides were 33-mers consisting of a central 10–23 catalytic domain (15 bp) flanked by target-specific binding arms (9 bp) (Fig. 1A). The sequence of the binding arms was arranged such that each deoxyribozyme would target a specific purine:uracil (RU) junction in the *E6* component of a long E6/E7 RNA substrate (Fig. 1B). Deoxyribozymes targeting the rat c-*myc* sequence were designed using the same approach except that molecules predicted to bind with a total free energy of hybridization ($\Delta G^\circ$) > –25 kcal/mol were excluded.

**Detection and analysis of *E6* multiplex deoxyribozyme cleavage.** To enable simultaneous analysis of multiple RNA cleavage sites along the entire *E6* target region of the E6/E7 transcript, three primer extension reactions were set up. The templates for these primer extensions were derived from in vitro transcribed E6/E7 RNA that had been exposed to a library of deoxyribozyme oligonucleotides (designed to target the segment of interest) in a multiplex cleavage reaction. The products from each labeled primer extension reaction were resolved on a DNA sequencing gel alongside the corresponding dideoxy sequencing ladder. The relative intensity of each band determined by densitometry gave an indication of the individual deoxyribozyme efficacy, and the sequencing ladder provided a reference for direct identification of the cleavage site. In addition to multiplex cleavage and sequencing products, a sample of primer extended target RNA that had been partially digested with RNase T1, was electrophoresed in parallel. Analysis of this partial digest provided an independent indicator of the prevailing secondary structure. In addition to primer extension at 45°C with reverse transcriptase, the

samples were also analyzed at high temperature (72°C) by extension with thermally stable Tth DNA polymerase. This produced the same profile of multiplex cleavage without the possibility of influence from deoxyribozyme oligonucleotides, which remain in solution.

To analyze large multiple reactions, deoxyribozyme concentrations ranging from 500 pM to 50 nM were found to be most effective. In this concentration range, the bands representing deoxyribozyme cleavage were distributed along the entire substrate as the primer extension analysis was capable of revealing the full spectrum of lesions (including the intact full-length target). This was an indication that there was usually one reaction event per target substrate molecule. To exclude the possibility of interference or cooperativity between different oligonucleotides within the multiplex cleavage reaction, the activity of each deoxyribozyme was also tested individually and compared with its corresponding activity in the combined reaction. The results demonstrated that, at low concentration, each deoxyribozyme in the multiplex reaction behaved independently with respect to the target substrate (data not shown).

To analyze the efficiency of each deoxyribozyme in the multiplex cleavage reaction, the intensity of each band from the sequencing gel (Fig. 2) was quantified and examined with respect to its position in the sequence. The most even distribution of deoxyribozyme cleavage was observed when the concentration of each oligonucleotide was 5 nM. At this or lower concentrations, only the most efficient deoxyribozymes in the mixed reaction are capable of producing a detectable signal, as they need to operate under stringent multiple-turnover conditions. At this level (5 nM), only 8 out of a total of 80 deoxyribozymes tested were able to maintain significant cleavage activity (Fig. 2). This concentration was probably ideal for the purpose of selecting efficient deoxyribozymes as it imposed concentration-dependent selection pressure and allowed an unbiased distribution of cleavage fragments for primer extension analysis. Under less stringent conditions (50 nM) the pattern and extent of deoxyribozyme activity on the complex substrate is more obvious (Fig. 2, lanes 4, 14, and 24). The clarity at this deoxyribozyme concentration comes at some expense of even distribution, with the normalized cleavage profile (and the intervening background) appearing to be slightly more intense at sites proximal to the primer binding site (Fig. 3).




**Figure 1. A schematic representation of the 10–23 general purpose RNA-cleaving DNA enzyme and the HPV16 E6/E7 target sequence. (A) The deoxyribozyme-substrate complex forms by Watson-Crick interactions between generic deoxyribonucleotides (N) in the arms of the deoxyribozyme (bottom) and the corresponding ribonucleotides (N) in the target (top). The defined 15-base sequence in the loop joining each arm represents the conserved catalytic motif and spans a single unpaired purine at the RNA target site. (B) The RNA sequence of the HPV16 E6/E7 bicistronic transcript showing potentially cleavable purine-uracil sites (bold U) in *E6* targeted by multiplex deoxyribozyme reactions. Arrows indicate the primer binding sites used for DNA template preparation and primer extension reactions. The underlined AUG motifs are at the E6 and E7 start codons, respectively.**

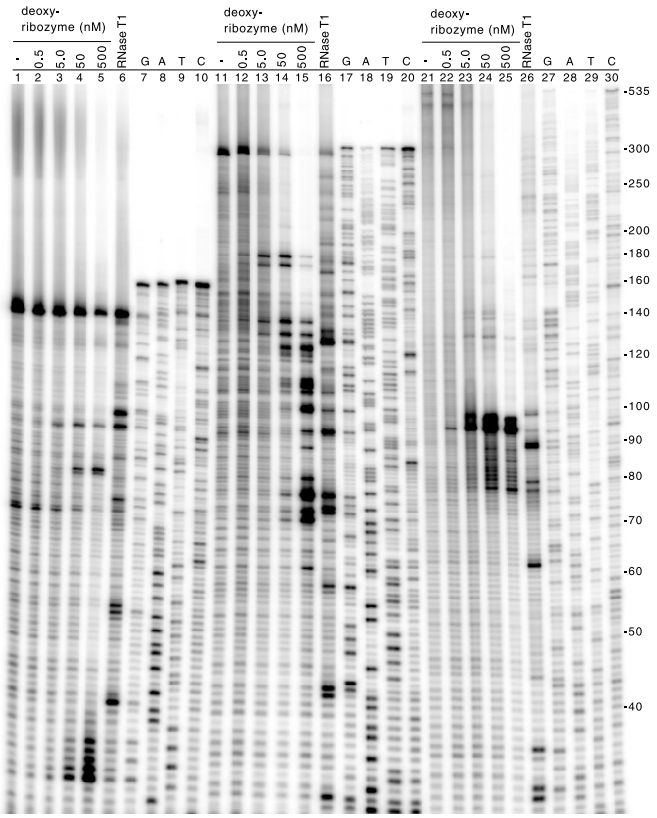


**Figure 2. Phosphorimage of a DNA sequencing gel containing the primer extension products of multiplex cleavage reactions in the E6/E7 transcript. Lanes 1–5: Cleavage reactions with 0, 0.5, 5, 50, and 500 nM concentrations, respectively, of deoxyribozyme oligonucleotides directed to the 5′ segment of the *E6* gene and revealed by extension of primer PE6A. Lane 6: Extension of the same primer on substrate RNA that had been subjected to partial digestion with RNase T1. Bands representing deoxyribozyme-induced cleavage in lanes 2–5 were positioned by direct alignment with the corresponding dideoxy sequencing reactions (lanes 7–10) also produced by the same primer. These extend slightly beyond the 5′ end of the corresponding RNA (lanes 1–6) as the template contains the T7 promoter sequence. Lanes 11–20 and 21–30 contain the same order of samples as described for lanes 1–10 except that they were derived from reactions directed to the middle and 3′ segments of *E6* and revealed by extension of primers PE6B and PE7A, respectively. The scale on the right indicates the molecular weight (bp) of the primer extension fragments.**

In addition to multiplex cleavage reactions, each experiment also contained a partial RNase T1 digestion of the substrate performed under the same conditions. This can be visualized in lanes 6, 16, and 26 of the sequencing gel (Fig. 2) and in the normalized digestion profile (Fig. 3A). When this was compared with the pattern of multiplex deoxyribozyme activity, sites hypersensitive to RNase digestion frequently colocalized with binding sites of efficient deoxyribozymes. This was particularly prominent in the case of DT99 (bp 540), which displayed outstanding performance and colocalized with three sites of RNase hypersensitivity (Fig. 2). Other sites where efficient deoxyribozyme activity correlated with a relative increase in RNase digestion could be seen by matching the intensity peaks between the two samples measured by densitometry (Fig. 3A and B). For example, the deoxyribozymes DT65–67 all bound in the same vicinity as the highly ribonuclease-sensitive site at position 273. Similarly, peaks of RNase activity at positions 132, 136, 188, 325, 553, and 556 also correlated with sites of efficient deoxyribozyme activity. However, this was not universal, as some positions amenable to RNase digestion did not contain active deoxyribozymes.

The positions of effective deoxyribozymes in the full-length target RNA tended to be clustered into groups (particularly in the 50 nM multiplex reaction) separated by regions containing low or unreactive sites (Figs. 2 and 3). In many cases, (e.g., between DT51–54, DT65–69, DT73–76 and DT107–109) relatively active target sites were very close or even overlapping. To gain some appreciation of the relationship between heteroduplex stability and cleavage activity, the $\Delta G^{o}$ was predicted for each deoxyribozyme (by the nearest neighbor method[10]) and charted in parallel to the cleavage intensity and RNase activity profiles (Fig. 3). From this analysis, we found that it was only deoxyribozyme-substrate heteroduplexes with a total $\Delta G^{o} < -20$ kcal/mol that demonstrated substantial cleavage activity in the long substrate.

Due to the length of the deoxyribozyme (33-mer), some oligonucleotides may have inhibited their own trans cleaving efficiency by forming stable intramolecular hairpin structures. There was some suggestion of this interference in DT75 (227 bp): Activity dropped sharply between this position and the two flanking deoxyribozymes DT74 and DT76. In contrast to the surrounding oligonucleotides,

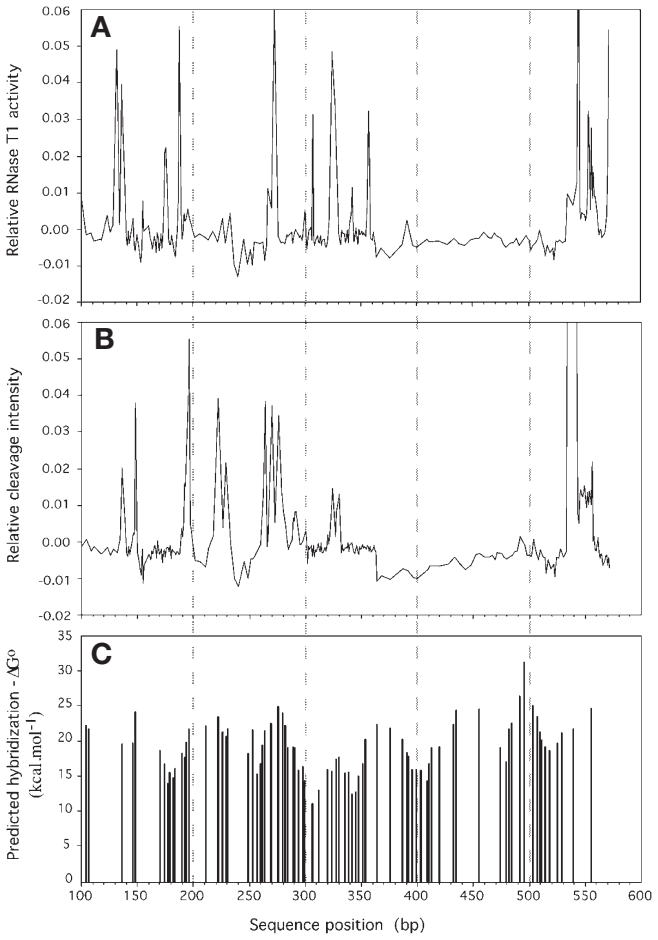


**Figure 3. Graph comparing the normalized intensity profile derived from densitometry of (A) a partial RNase T1 digestion of the substrate, (B) the 50 nM multiplex deoxyribozyme reaction, and (C) the predicted total $\Delta G^{o}$ for each deoxyribozyme-substrate heteroduplex. Each of these parameters was aligned in parallel and with respect to the sequence position in the long E6/E7 transcript.**

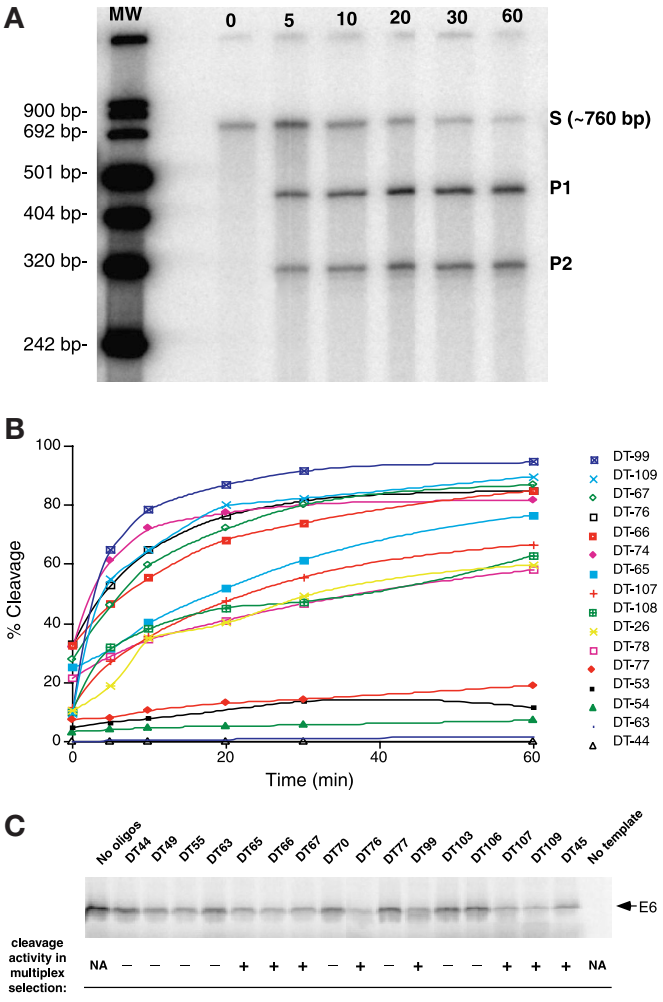


**Figure 4. Analysis of E6 deoxyribozyme-mediated target RNA cleavage and cell-free translation. (A) Deoxyribozyme (DT99) cleavage of the E6/E7 transcript over 1 h. The reaction time (min) and molecular weight are indicated at the top and left side of the gel, respectively. The position of the unreacted substrate (S) and products (P1 and P2) are indicated. (B) The reaction progress was expressed graphically for DT99 (above) and another 12 deoxyribozyme molecules selected through multiplex reactions, as well as three deoxyribozymes that were not selected (DT44, 63, and 77). (C) The *E6* gene driven by a T7 promoter was transcribed and translated in a single tube system in the presence of deoxyribozymes, and the protein was resolved by electrophoresis. The identity of each deoxyribozyme used is indicated at the top of each lane and underneath its relative cleavage activity in the multiplex cleavage assay denoted as either more active (+) of less active (-).**

**Table 1. Summary of kinetic data[a].**

| Deoxyribozyme | Sequence | Cleavage site (bp) | ΔG° internal (kcal/mol) | ΔG° duplex (kcal/mol) | %P (1 h) | $k_{obs}$ ($min^{-1}$) |
|---|---|---|---|---|---|---|
| DT99 | GTTTCTCTAggctagctacaacgaGTGTTCTTG | 540 | 0.4 | –22.0 | 95 | 0.21 |
| DT74 | AAAGTCATAggctagctacaacgaACCTCACGT | 229 | –0.8 | –20.8 | 70 | 0.19 |
| DT109 | GTCCACCGAggctagctacaacgaCCCTTATAT | 492 | 0.9 | –26.7 | 90 | 0.15 |
| DT76 | TATACCTCAggctagctacaacgaGTCGCAGTA | 222 | 1.4 | –23.7 | 81 | 0.08 |
| DT67 | CCATCTCTAggctagctacaacgaATACTATGC | 264 | 1.8 | –21.7 | 84 | 0.07 |
| DT66 | GGATTCCCAggctagctacaacgaCTCTATATA | 270 | 1.4 | –22.7 | 80 | 0.05 |
| DT107 | ATACATCGAggctagctacaacgaCGGTCCACC | 504 | 1.4 | –25.3 | 67 | 0.05 |
| DT108 | ACCGGTCCAggctagctacaacgaCGACCCCTT | 496 | 0.7 | –31.5 | 63 | 0.06 |
| DT65 | GCATATGGAggctagctacaacgaTCCCATCTC | 276 | 0.2 | –25.2 | 72 | 0.03 |
| DT26 | CTCTGTGCAggctagctacaacgaAACTGTGGT | 148 | 0.9 | –24.3 | 60 | 0.05 |
| DT78 | CTTGCAGTAggctagctacaacgaACACATTCT | 196 | 1.1 | –22.0 | 46 | 0.02 |
| DT53 | CTATACTCAggctagctacaacgaTAATTTTAG | 324 | 1.6 | –15.9 | 12 | 0.07 |
| DT77 | TCGCAGTAAggctagctacaacgaTGTTGCTTG | 211 | 0.1 | –22.4 | 19 | 0.02 |
| DT54 | ACTCACTAAggctagctacaacgaTTTAGAATA | 320 | 1.6 | –16.2 | 7 | 0.02 |
| DT63 | CATACAGCAggctagctacaacgaATGGATTCC | 282 | –0.4 | –22.5 | 2 | 0.02 |
| DT44 | GTTGTTCCAggctagctacaacgaACAAACTAT | 354 | –2.8 | –20.4 | 0 | 0 |

[a]The name, sequence, site of cleavage, rate constants, and reaction extents over 1 h are shown for 13 deoxyribozymes selected by multiplex cleavage analysis, as well as three that were not selected. The predicted ΔG° values for an intramolecular structure (internal) and the total ΔG° for duplex formation between the deoxyribozyme arms and the target RNA are also shown. The 10–23 catalytic motif is indicated in lowercase and the sequence for the target binding domains are in uppercase.



this molecule was predicted to form a very stable stem loop structure with a ΔG° value of -2.0 kcal/mol and a melting temperature (Tm) of 60°C. Other molecules approaching or exceeding this level of internal stability had no measurable RNA cleavage activity.

**Kinetic analysis of selected *E6* cleaving deoxyribozymes.** The reaction rate of 13 active and three less active deoxyribozymes (identified in the 5 and 50 nM multiplex reactions) were examined individually under single-turnover conditions. This was achieved by incubating a labeled E6/E7 substrate for various time intervals up to 1 h with an excess of the deoxyribozyme. The progress of these reactions was followed by densitometry and the percentage product plotted against time (Fig. 4B). In each case the values for $k_{obs}$ (determined by regression analysis of the progress curves) and reaction extent, largely reflected the observation in the multiplex reactions (Table 1). The most impressive deoxyribozymes in the multiplex reaction also demonstrated exceptional kinetic activity under single-turnover conditions. This was exemplified by DT99 (540 bp), which was able to cleave approximately 80% of the substrate transcript in 10 min (95% over 1 h) with a first order rate constant ($k_{obs}$) of 0.21/min. Other selected deoxyribozymes also performed well against the long transcript under single-turnover conditions, particularly oligonucleotides DT74 (229 bp) and DT109 (492 bp). However, despite the potency of these molecules, it was surprising how rapidly the activity of each deoxyribozyme declined when descending through the list (Table 1). This is apparent in the case of DT54, which ranked in the top 20% of molecules in both the 5 nM and 50 nM multiplex reactions and yet could cleave only about 7% of the substrate in 1 h with a $k_{obs}$ value of 0.02/min. Indeed, a large proportion of these deoxyribozymes (>65%) had no appreciable activity at all. Under these conditions, only 10% of potentially cleavable (RU) sites in the E6/E7 transcript were actually cleaved substantially by a 10–23 deoxyribozyme at 5 nM concentration. Sites chosen at random could therefore be considered to have a 90% chance of failure at this concentration.

**Deoxyribozyme suppression of gene expression in a cell-free system.** To examine the potential of deoxyribozymes (selected by in vitro cleavage) for inhibiting target gene expression, a coupled transcription/translation system was established. In this cell-free assay, the production of $^{35}$S-methionine-labeled E6 protein from a double-stranded DNA template was monitored in the presence of eight active and eight less active deoxyribozymes. The relative concentration of the products resolved by SDS-PAGE (Fig. 4C) demonstrated that all

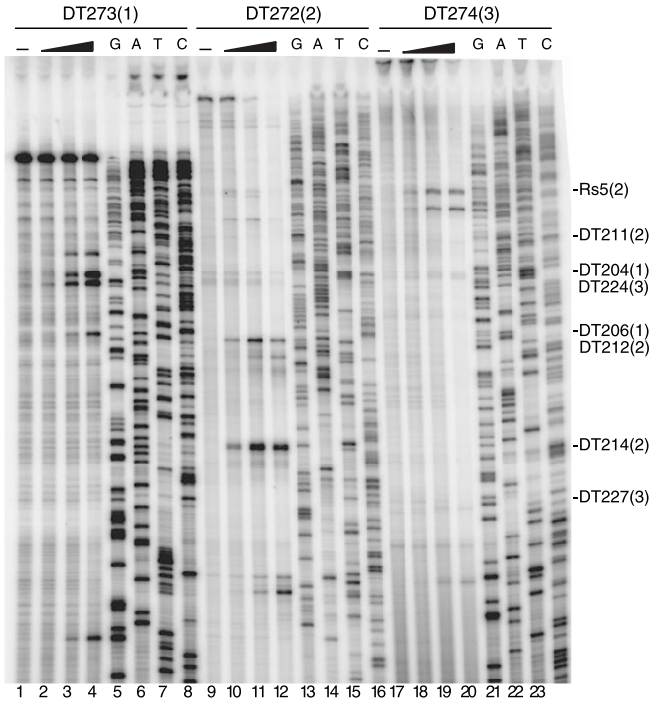


**Figure 5. Multiplex selection of c-*myc*–cleaving deoxyribozymes. Phosphorimage of a DNA-sequencing gel resolving the primer extension products of a multiplex deoxyribozyme cleavage reaction in a rat c-*myc* RNA transcript. Lanes 1–4: multiplex reactions in the 5′ terminal segment, with 0, 5, 50, and 500 nM concentrations of deoxyribozymes, respectively (denoted by [-] and ramp). Lanes 5–8: The corresponding sequencing ladder produced with the same primer as lanes 1–4. Lanes 9–16 and 17–24 were similar to lanes 1–8 except they were derived from reactions in the downstream segments of the target and were revealed by primers with binding activity further downstream. The target sites of deoxyribozymes chosen for analysis in the SMC proliferation assay (Fig. 6) are indicated on the right, with the respective segment (1, 2, or 3) in brackets.**

eight deoxyribozymes characterized by high levels of transcript cleavage in vitro also exhibited substantial inhibition of E6 protein synthesis, whereas the less active molecules showed only a marginal effect. This was highlighted by three of the most efficient E6 cleavers (DT99,

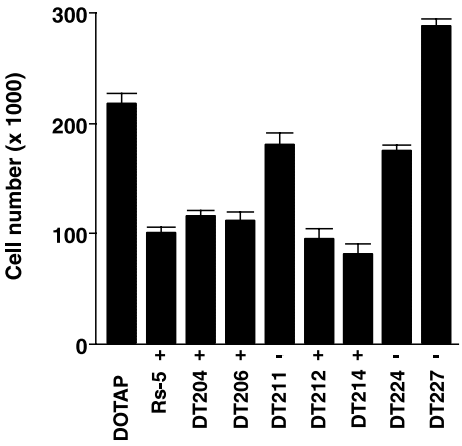


**Figure 6. Deoxyribozyme-mediated suppression of SMC proliferation. Five *c-myc*–cleaving (+) and noncleaving (-) deoxyribozymes selected in a multiplex assay were compared for their ability to suppress SMC proliferation. Growth suppression is indicated by number of cells after treatment with each deoxyribozyme, and a control treatment without deoxyribozyme (DOTAP).**

DT109, and DT76; see Table 1), which performed even better in the cell-free system than the other deoxyribozymes in the active group. In contrast, the three weakest deoxyribozymes (DT44, DT63, and DT77) had the least effect on E6 protein synthesis.

**The influence of *c-myc*–cleaving deoxyribozymes on smooth muscle cell proliferation.** To evaluate the biological activity of deoxyribozymes selected on the basis of their cleavage efficiency, we compared the activity of c-*myc*–cleaving deoxyribozymes in a multiplex assay for their effect on vascular smooth muscle cell (SMC) proliferation. The multiplex cleavage assay was performed on a full-length (2.2 kb) Rat c-*myc* transcript, using RU-cleaving deoxyribozymes with a □G°<–25 kcal/mol. The cleavage reaction profile for the first 1 kb of the target was obtained by three primer extension reactions and resolved by sequencing gel electrophoresis (Fig. 5). Efficient and poor c-*myc* cleavers were compared for their ability to suppress myc-related SMC proliferation. The cell counts of deoxyribozyme-treated SMCs provided an indication of the respective biological response[11] (Fig. 6). These observations, particularly in the case of DT214, demonstrated that the efficient c-*myc* cleavers in vitro also induce the most substantial suppression of SMC proliferation. In contrast, the poor c-*myc* cleavers had little or no effect on the level of SMC proliferation.

## Discussion

The greatest obstacle for deoxyribozymes and other agents that bind their target by Watson-Crick base pairing is the underlying RNA secondary structure. Even knowing the location of unpaired loops does not guarantee effective hybridization because of unpredictable steric and topological constraints[7,12]. In this study we have demonstrated a method for determining which deoxyribozymes are successful in cleaving a complex RNA molecule regardless of secondary structure. In the *HPV16 E6* component of the E6/E7 transcript, we systematically compared 80 deoxyribozymes using this method, and found approximately 10% to be very effective at cleaving the target. Many of the efficient deoxyribozymes were clustered in overlapping sites, which indicated shared regions of accessibility, possibly occurring at an RNA stem loop or single-stranded bulge. Active deoxyribozymes in many instances colocalized with sites of RNase T1 hypersensitivity. These sites of preferential digestion have a tendency to occur at unpaired guanine residues and provided an independent indication of target RNA secondary structure. Although this supported the belief that the RNA secondary structure is an important determinant of deoxyribozyme activity in a long substrate, its predictive value was limited in that ribonuclease-sensitive regions were not always cleaved efficiently by the corresponding deoxyribozymes.

In addition to target-site accessibility, the thermodynamics of enzyme-substrate interactions also strongly influence the efficiency of deoxyribozyme-mediated hydrolysis of a long RNA. In short substrates lacking secondary structure, the kinetic activity of different deoxyribozymes of equal length varies substantially from one sequence to another. This sequence-dependent variation can often be predicted in terms of ΔG° or measured empirically as differences in Tm. The main influence over the stability of a DNA/RNA heteroduplex, as in the case of a homoduplex, is the guanosine cytidine content[10]. In addition, heteroduplex formation has been shown to be more favorable when the deoxyribonucleotide strand is pyrimidine-rich (i.e., the stability of dY-rR > dR-rY)[13,14].

The efficiency of deoxyribozymes with low activity (characterized by relatively high predicted ΔG° values) can usually be improved significantly by increasing the length of the target binding arms. This improvement, which is related to increased substrate affinity, has been demonstrated previously by a decrease in the value of the kinetic parameter $K_M$ (ref. 1). For convenience, we arbitrarily designed deoxyribozymes with symmetric nine-base arms. At some sites, this length may not have been adequate to achieve the heteroduplex stability required for efficient cleavage. In an alternative strategy, when the predicted ΔG° for a given arm sequence is too high (>–20 kcal/mol), additional nucleotides are added to reduce it to a level that is indicative of a stable complex. Modified nucleotide analogs that display higher affinity for RNA could also be used in the deoxyribozyme-binding arms, such that further increases in length are not required. For example 2′O methyl derivatives have been shown to bind RNA with higher affinity than normal deoxynucleotides and to have increased resistance to nucleases[15,16]. Conversely, it should be noted that when DNA modification reduces oligonucleotide affinity for RNA, such as with phosphorothioate linkages, it would also be necessary to compensate the deoxyribozyme by increasing the arm length in order to retain the desired activity (data not shown).

Our analysis of thermodynamic stability confirmed that active deoxyribozymes usually demonstrated above-average affinity for their target RNA. However, favorable ΔG° values for hybridization alone could not be used to select effective deoxyribozymes, as they were not sufficient to predict cleavage in the long substrates. Interestingly, deoxyribozymes that maintained their activity at low concentrations had higher predicted thermodynamic stability than those with activity that was only apparent at high concentrations. This probably indicates that the deoxyribozymes with greater target affinity also display greater kinetic efficiency under multiple-turnover conditions because of a correspondingly lower $K_M$.

While the cleavage of full-length RNA under simulated physiologic conditions in vitro is a valuable indicator of catalytic nucleic acid activity, its correlation with gene suppression in vivo appears to vary significantly from one system to another. This probably is caused by competition for oligonucleotide binding sites by proteins in the cellular environment, or by unfavorable rearrangements of the RNA secondary structure. Other factors that may decrease their biological activity in vivo include poor cellular uptake or colocalization with the target. To address these issues, we adopted a cell-free system to validate the selection of E6 deoxyribozymes on the basis of in vitro cleavage. This model has the advantage of simulating the interactions between the transcriptional and translational machinery, the nascent RNA target, and the deoxyribozyme, and avoids the uncertainty associated with cellular uptake and intracellular trafficking of oligonucleotides. For these and other reasons, this system has been

used to simulate in vivo conditions for antisense/ribozyme[17,18] and conventional drug screens.

The correlation between deoxyribozyme-mediated suppression of *E6* gene expression in this system (Fig. 4C) and RNA cleavage activity in vitro, indicated that the multiplex screening approach could be used to generate a short list of effective deoxyribozymes to evaluate further in a cellular environment. To explore the potential value of in vitro target-site selection for revealing deoxyribozymes with intracellular activity, we compared the cleavage activity of anti–c-*myc* deoxyribozymes in a multiplex assay for their effect on SMC proliferation. The results showed a surprisingly high correlation between the efficiency of in vitro cleavage and suppression of SMC proliferation in culture.

In summary, deoxyribozyme efficiency in a long substrate depends on a combination of both secondary structure and hybridization thermodynamics. The difficulty in predicting the former is that many target sites must be tested empirically to determine the most efficient molecules. Although this task is very time-consuming (if target sites are analyzed one by one), we observed that only 10% of possible sites in the E6/E7 RNA were readily cleaved by a 10-23 deoxyribozyme. Fortunately, this process can be multiplexed in a convenient assay that allows simultaneous analysis of many cleavage sites at a broad range of deoxyribozyme concentrations. This streamlined approach offers the possibility of direct comparison of all sites for a given target in a single reaction. In our experience this information is also relevant to the biological activity of deoxyribozymes and may thus be useful in both therapeutic applications and target validation.

## Experimental protocol

**Oligonucleotides**. Oligonucleotides were purchased from Oligos, Etc. (Wilsonville, OR) and Beckman Instruments (Sydney, Australia). All deoxyribozymes were constructed using the 10-23 catalytic motif [ggctagctacaacga][1] and 9 bp hybridizing arms specific for each site along the target RNA transcript. Each deoxyribozyme oligonucleotide was designed to target RU junctions in either the E6 segment of the E6/E7 transcript (Fig. 1B) or the rat c-*myc* transcript. Purine-cytosine sites also cleavable by the 10–23 deoxyribozyme were ignored in this study as these positions have been shown to be generally less reactive (data not shown). The sequence and binding site of primer oligonucleotides used for DNA template preparation and primer extension analysis were as follows (see also Fig. 1B). Template preparation for the E6/E7 sequence was achieved by PCR with forward and reverse primers of sequence: 5′-TTATACGACTCACTATAGGGAGAACTGCAATGTTTCAGGAC-3′ (PE6T7: bp 94–115) and 5′-GATTATGGTTTCTGAGAACAG-3′ (PE7REV: bp 860–839). Primer extension was accomplished with 5′-CCTCACGTCGCAGTAACTGTTGCTTGC-3′ (PE6A: bp 237–201), 5′-ATCACACAACGGTTTGTTGTATTGCTG-3′ (PE6B: bp 397–371), and 5′-CAGTAGAGATCAGTTGTCTCTGGTTGC-3′ (PE7A: bp 632–606). Template for the rat c-*myc* sequence was generated by primers with sequence: 5′-TTATACGACTCACTATAGGGAGACTCGCTGTAGTAATTCCAGCGAGAGACAG-3′ (DT197: bp 1–30) and 5′-TGGCTCAATTATTTTTTCCAATTAT-3′ (DT196: bp 2168–2141); primer extension analysis was achieved with oligonucleotides of sequence 5′-CAGCTGATCGGCGGTGGAGAAGTTG-3′ (DT272: bp 713–688), 5′-TTCAGGCTTCAAATAACGCGAGGAG-3′ (DT273: bp 376–351), 5′-GCTGTCGTTGAGCGGGTAGGGGAAG-3′ (DT274: bp 1022–997).

**In vitro transcription.** Linear template DNA for the production of an E6/E7 transcript was prepared by PCR in a mixture containing 10 pM plasmid DNA (designated pHPV16) containing an HPV16 genomic insert (American Type Culture Collection [ATCC] 45113). The consensus T7 phage promoter sequence was introduced to the coding strand of the amplicon in the forward primer (PE6T7) specific for the E6 5′-untranslated and translation-initiation region. The reverse primer (PE7REV) was designed to anneal to the 3′ end of the E7 gene. The reaction was carried out in a solution containing 16.6 mM $(NH_4)_2SO_4$, 67 mM Tris-HCl, pH 8.8, 6.7 mM $MgCl_2$, 0.87 U Ampli*Taq* DNA polymerase (Perkin-Elmer, Foster City, CA) 300 μM each of dGTP, dATP, dTTP, and dCTP, and 50 pmol of each oligonucleotide primer. After 25 temperature cycles at 95°C for 30 s, 60°C for 90 s, and 72°C for 60 s, the products were purified by electrophoresis in a 2% agarose gel and extracted from the agarose with Gene Clean (Bio 101, Vista, CA). Template DNA used for the synthesis of a full-length rat c-*myc* transcript was produced by a similar strategy except that the c-*myc* cDNA was derived directly from reverse transcription PCR of purified mRNA from rat smooth muscle cells.

For the production of unlabeled RNA, in vitro transcription was performed with 100 ng purified template DNA and T7 RNA polymerase at 37°C for 3 h using an RNA transcription kit (Epicentre Technology, Madison, WI). A $^{32}$P-labeled transcript (for kinetic analysis) was synthesized on the same template DNA by transcription in the presence of [□-$^{32}$P]UTP (Bresatec, Adelaide, Australia). The reagents and T7 RNA polymerase for this reaction were supplied in another RNA transcription kit (Stratagene, La Jolla, CA).

**Deoxyribozyme cleavage reactions**. Multiple or individual deoxyribozyme oligonucleotides (0.5 nM–0.5 μM) and synthetic RNA substrate (0.2 μM) were pre-equilibrated separately for 10 min at 37°C in equal volumes of 50 mM Tris-HCl, pH 7.5, 10 mM $MgCl_2$, 150 mM NaCl, and 0.01% SDS. The reaction was initiated by mixing the deoxyribozyme(s) and substrate together. After 1 h the reactions were stopped by emersion in ice and precipitated in ethanol.

**Partial RNase digestion.** The E6/E7 transcript (0.2 μM) was subjected to partial digestion with RNase T1 (0.2–1.0 U) in 50 mM Tris-HCl, pH 7.5, 10 mM $MgCl_2$, and 150 mM NaCl for 10 min at 37°C. The reactions (20 μl) were stopped by extraction in 100 μl of phenol/chloroform and recovered by ethanol precipitation.

**Primer extension.** Each primer (1 μM) was radiolabeled at the 5′-terminal in 60 mM Tris-HCl, pH 7.5, 9 mM $MgCl_2$, 10 mM dithiothreitol, 1 U polynucleotide kinase (New England Biolabs, Beverly, MA) and 10 μCi of [□-$^{32}$P]ATP (Bresatec) at 37°C for 30 min and 75°C for 5 min. Primer extension analysis was performed on deoxyribozyme-cleaved and ribonuclease-digested RNA using either SuperScriptII reverse transcriptase (Life Technologies, Gaithersburg, MD) or thermally stable Tth DNA polymerase (Promega, Madison, WI). In each reaction, 2 pmol labeled primer was combined with 400 nM of RNA and denatured at 90°C for 5 min. For extension with superscript reverse transcriptase, the primer was allowed to anneal slowly between 45–65°C before adding the first strand buffer, dithiothreitol, deoxyribonucleotides, and enzyme (according to the manufacturer's instructions). This mixture (final volume, 20 μl) was incubated for 1 h at 45°C before being transferred to ice. Alternatively, after annealing at 65°C for 5 min, extension was achieved at 72°C with Tth DNA polymerase over 20 min. These reactions contained Tth polymerase buffer supplemented with $MnCl_2$ (in accordance with the manufacturer's instructions) for use with an RNA template. In this protocol the entire 20 μl reaction volume (including enzyme and dNTPs) was assembled on ice prior to the thermal denaturation step. Sequencing fragments corresponding to each segment of the target were also generated by primer extension on the double-stranded DNA template in the presence of chain-terminating dideoxynucleotides (ddNTP). In these four reactions the dNTP concentration was reduced to 2.5 μM while being supplemented by either 10 μM ddGTP, 100 μM ddATP, 200 μM ddTTP, or 100 μM ddCTP in 16.6 mM$(NH_4)_2SO_4$, 67 mM Tris-HCl, pH 8.8, 6.7 mM $MgCl_2$, 0.87 U Ampli*Taq* DNA polymerase (Perkin Elmer Cetus) and 1.0 pmol of the $^{32}$P-labeled oligonucleotide. This reaction was performed as a linear amplification over 25 temperature cycles at 95°C for 30 s, 60°C for 90 s, and 72°C for 60 s (ref. 19).

**Densitometry**. After primer extension, samples were combined with equal volumes of stop buffer (formamide, EDTA, loading dye) before electrophoresis on a 6% denaturing polyacrylamide gel. The corresponding image was revealed and the band intensity quantified at each position with a Phosphorimager and ImageQuant software (Molecular Dynamics, Sunnyvale, CA). The relative intensity of cleavage bands as a proportion of the total lane intensity was used to construct a normalized profile of deoxyribozyme and RNase activity.

**Deoxyribozyme kinetics.** Deoxyribozyme oligonucleotides that demonstrated superior activity in multiplex cleavage reactions were also compared with other deoxyribozymes showing less activity by more conventional analysis of single-turnover kinetics. In this assay a full-length $^{32}$P-labeled E6/E7 transcript (prepared by in vitro transcription) was incubated with a 10-fold excess of individual deoxyribozyme oligonucleotide (1 μM) at 37°C for 0, 5, 10, 20, 30, and 60 min. The reaction conditions, electrophoresis, and analysis of these deoxyribozyme cleavage reactions were otherwise the same as described above. The percentage of band intensity volume in the cleavage products were then analyzed graphically in a plot against time. A curve was generated for the data (least-squares) using the equation $\%P = \%P_\infty - C \cdot \exp[-kt]$ where %P is the percentage product, $\%P_\infty$ is the percentage product at $t = \infty$, C is the difference in %P between $t = \infty$ and $t = 0$, and k is the first order rate

constant[20]. The first order rate constant ($k_{obs}$) was used to compare the rates of different deoxyribozymes.

**Cell-free transcription/translation assay.** Deoxyribozyme-mediated suppression of target gene expression was examined in a coupled cell-free transcription/translation system. E6 protein synthesis was monitored in the presence of various deoxyribozymes classified as either efficient or inefficient on the basis of their cleavage activity in the multiplex assay. This was accomplished in a single tube (Novagen, Madison, WI) system according to the manufacturer's instructions with the addition of deoxyribozyme oligonucleotides. Briefly, 0.5 µg of *E6* template DNA encompassing a T7 promoter was incubated with 4 µl transcription mixture, 15 µl of translation mixture, 1 µl of $^{35}$S-methionine (1000 µCi/mmol; Amersham, Buckinghamshire, UK) and 1 µM deoxyribozyme oligonucleotides in a final volume of 25 µl. After 60 min at 30°C the reaction was then incubated for a further 5 min at room temperature with 1 µl of RNase A (10 mg/ml) to remove the charged tRNA. A 5 µl aliquot from each sample was then combined with 20 µl of loading buffer (10% glycerol, 2% SDS, 62.5 mM Tris-HCl, pH 6.8, 0.02% bromophenol blue) and heated to 95°C for 5 min before electrophoresis on an SDS protein gel. After electrophoresis, the gel was fixed in 10% TCA and dried under vacuum, and the image was recovered by a phosphorimager.

**SMC proliferation assay.** Rat SMCs (SV40LT-SMC, ATCC CRL 2018) were grown at 33°C with 5% $CO_2$ in Dulbecco's modified Eagle's medium supplemented with 10% calf serum and 200 µg/ml of G418. For proliferation analysis, cells were transferred to six-well cluster plates and allowed to attach overnight. They were then washed twice with phosphate-buffered saline and grown in 0.25% calf serum/DMEM for a period of 4 days at 33°C. The low serum media [was then replaced with 10% calf serum/DMEM and the deoxyribozyme oligonucleotides (1 µM)/DOTAP transfection reagent was added as triplicate samples. After 3 days cells were harvested with trypsin and quantified in a Coulter counter.


1. Santoro, S.W. & Joyce, G.F. A general purpose RNA-cleaving DNA enzyme. *Proc. Natl. Acad. Sci. USA* **94,** 4262–4266 (1997).
2. Milner, N., Mir, K.U. & Southern, E.M. Selecting effective antisense reagents on combinatorial oligonucleotide arrays. *Nat. Biotechnol*. **15,** 537–541 (1997).
3. Lima, W.F., Brown-Driver, V., Fox, M., Hanecak, R. & Bruice, T.W. Combinatorial screening and rational optimization for hybridization to folded hepatitis C virus RNA of oligonucleotides with biological antisense activity. *J. Biol. Chem.* **272,** 626–638 (1997).
4. Birikh, K.R., Berlin, Y.A, Soreq, H. & Eckstein, F. Probing accessible sites for ribozymes on human acetylcholinesterase RNA. *RNA* **3,** 429–437 (1997).
5. Ho, S.P. et al. Potent antisense oligonucleotides to the human multidrug resistance-1 mRNA are rationally selected by mapping RNA-accessible sites with oligonucleotide libraries. *Nucleic Acids Res.* **24,** 1901–1907 (1996).
6. Ho, S.P. et al. Mapping of RNA accessible sites for antisense experiments with oligonucleotide libraries. *Nat. Biotechnol*. **16,** 59–63 (1998).
7. Matveeva, O., Felden, B., Audlin, S., Gesteland, R.F. & Atkins, J.F. A rapid *in vitro* method for obtaining RNA accessibility patterns for complementary DNA probes: correlation with an intracellular pattern and known RNA structures. *Nucleic Acids Res.* **25,** 5010–5016 (1997).
8. Lieber, A. & Strauss, M. Selection of efficient cleavage sites in target RNAs by using a ribozyme expression library. *Mol. Cell Biol*. **15,** 540–55 (1995).
9. Campbell, T.B. & Cech, T.R. Identification of ribozymes within a ribozyme library that efficiently cleave a long substrate RNA. *RNA* **1,** 598–609 (1995).
10. Sugimoto, N. et al. Thermodynamic parameters to predict stability of RNA/DNA hybrid duplexes. *Biochemistry* **34,** 11211–11216 (1995).
11. Simons, M., Edelman, E.R. & Rosenberg, R.D. Antisense proliferating cell nuclear antigen oligonucleotides inhibit intimal hyperplasia in a rat carotid artery injury model. *J. Clin. Invest.* **93,** 2351–2356 (1994).
12. Lima, W.F., Monia, B.P., Ecker, D.J. & Freier, S.M. Implication of RNA structure on antisense oligonucleotide hybridisation kinetics. *Biochemistry* **31,** 12055–12061 (1992).
13. Ratmeyer, L., Vinayak, R., Zhong, Y.Y., Zon, G. & Wilson, W.D. Sequence specific thermodynamic and structural properties for DNA•RNA duplexes. *Biochemistry* **33,** 5298–5304 (1994).
14. Gyi, J.I., Lane, A.N., Conn, G.L. & Brown, T. Solution structures of DNA•RNA hybrids with purine-rich and pyrimidine rich strands: Comparison with homologous DNA and RNA duplexes. *Biochemistry* **37,** 73–80 (1998).
15. Inoue, H. et al. Synthesis and hybridization studies on two complementary nona(2′-O-methyl)ribonucleotides. *Nucleic Acids Res.* **15,** 6131–6148 (1987).
16. Majlessi, M., Nelson, N.C. & Becker, M.M. Advantages of 2′-O-methylribonucleotide probes for detecting RNA targets. *Nucleic Acids Res.* **26,** 2224–2229 (1998).
17. Bielinska, A., Kukowska-Latallo, J.F., Johnson, J., Tomalia, D.A. & Baker, J.R. Jr. Regulation of *in vitro* gene expression using antisense oligonucleotides or antisense expression plasmids transfected using starburst PAMAM dendrimers. *Nucleic Acids Res.* **24,** 2176–2182 (1996).
18. Le Tinevez, R., Mishra, R.K. & Toulme, J.J. Selective inhibition of cell-free translation by oligonucleotides targeted to a mRNA hairpin structure. *Nucleic Acids Res.* **26,** 2273–2278 (1998).
19. Murray, V. Improved double-stranded DNA sequencing using the linear polymerase chain reaction. *Nucleic Acids Res.* **17,** 8889 (1989).
20. Hendry, P., McCall, M.J., Santiago, F.S. & Jennings, P.A. A ribozyme with DNA in the hybridising arms displays enhanced cleavage ability. *Nucleic Acids Res.* **21,** 5737–5741 (1992).